The Astrophysical Journal Letters, 791:L30 (6pp), 2014 August 20 doi:10.1088/2041-8205/791/2/L30

HST-COS SPECTROSCOPY OF THE COOLING FLOW IN A1795—EVIDENCE FOR INEFFICIENT STAR FORMATION IN CONDENSING INTRACLUSTER GAS

Michael McDonald[1,6], Joel Roediger[2,3], Sylvain Veilleux[4,5], and Steven Ehlert[1]
[1] Kavli Institute for Astrophysics and Space Research, MIT, Cambridge, MA 02139, USA; mcdonald@space.mit.edu
[2] Department of Astronomy, University of California Santa Cruz, CA 95064, USA
[3] Department of Physics, Engineering Physics, & Astronomy, Queen's University, Kingston, Ontario, Canada
[4] Department of Astronomy, University of Maryland, College Park, MD 20742, USA
[5] Joint Space-Science Institute, University of Maryland, College Park, MD 20742, USA
Received 2014 May 30; accepted 2014 July 15; published 2014 August 6

ABSTRACT

We present far-UV spectroscopy from the Cosmic Origins Spectrograph on the *Hubble Space Telescope* of a cool, star-forming filament in the core of A1795. These data, which span 1025 Å $< \lambda_{\rm rest} <$ 1700 Å, allow for the simultaneous modeling of the young stellar populations and the intermediate-temperature ($10^{5.5}$ K) gas in this filament, which is far removed (∼30 kpc) from the direct influence of the central active galactic nucleus. Using a combination of UV absorption line indices and stellar population synthesis modeling, we find evidence for ongoing star formation, with the youngest stars having ages of $7.5^{+2.5}_{-2.0}$ Myr and metallicities of $0.4^{+0.2}_{-0.1}$ $Z_{\odot}$. The latter is consistent with the local metallicity of the intracluster medium. We detect the O VI λ1038 line, measuring a flux of $f_{\rm O\,VI,1038} = 4.0 \pm 0.9 \times 10^{-17}$ erg s^{-1} cm^{-2}. The O VI λ1032 line is redshifted such that it is coincident with a strong Galactic H_2 absorption feature, and is not detected. The measured O VI λ1038 flux corresponds to a cooling rate of 0.85 ± 0.2 (stat) ± 0.15 (sys) $M_{\odot}$ yr^{-1} at $\sim 10^{5.5}$ K, assuming that the cooling proceeds isochorically, which is consistent with the classical X-ray luminosity-derived cooling rate in the same region. We measure a star formation rate of 0.11 ± 0.02 $M_{\odot}$ yr^{-1} from the UV continuum, suggesting that star formation is proceeding at 13^{+3}_{-2}% efficiency in this filament. We propose that this inefficient star formation represents a significant contribution to the larger-scale cooling flow problem.

Key words: galaxies: clusters: individual (A1795) – galaxies: clusters: intracluster medium – galaxies: star formation – galaxies: stellar content

Online-only material: color figures

1. INTRODUCTION

In the cores of galaxy clusters, the intracluster medium (ICM) can reach high enough density and low enough temperature that the inferred cooling time is much shorter than the age of the universe. In these so-called "cooling flow clusters," simple models predict that ∼100–1000 $M_{\odot}$ yr^{-1} of cool gas should condense out of the hot intracluster plasma and fuel star formation in the central cluster galaxy (for a review, see Fabian 1994). However, with few notable exceptions (McNamara et al. 2006; McDonald et al. 2012a), we do not observe such vigorous starbursts at the centers of galaxy clusters: the typical star formation rate in the core of a cooling flow cluster is only ∼1–10 $M_{\odot}$ yr^{-1} (e.g., Hicks & Mushotzky 2005; O'Dea et al. 2008; McDonald et al. 2011). This low level of star formation is most likely being fueled by local thermodynamic instabilities in the ICM (e.g., McCourt et al. 2012), with the remaining $\gtrsim$90% of the energy lost from cooling being offset by radio-mode feedback from the central active galactic nucleus (AGN; e.g., Churazov et al. 2001; Rafferty et al. 2006, 2008; Fabian 2012; McNamara & Nulsen 2012).

While most cooling flow clusters show evidence of such "reduced cooling flows" in the form of ongoing star formation (e.g., Johnstone et al. 1987; McNamara & O'Connell 1989; Allen 1995; O'Dea et al. 2008; Hicks et al. 2010; McDonald et al. 2011) and cold molecular gas (e.g., Edge 2001; Edge et al. 2002; Salomé & Combes 2003; Hatch et al. 2005; Salomé et al. 2011; McDonald et al. 2012c), there is still very little evidence for gas between 10^4 K and 10^7 K, which would directly link the hot and cool phases. High-resolution X-ray spectroscopy of individual clusters has, thus far, only been able to put upper limits on the amount of ∼10^6 K gas in the cores of galaxy clusters (e.g., Peterson et al. 2003; Peterson & Fabian 2006; Sanders et al. 2010). Recently, Sanders & Fabian (2011) performed a stacking analysis of X-ray grating spectra, yielding a detection of O VII at a level ∼4–8 times lower than the expectation from simple cooling flow models. Using the *FUSE* satellite, Oegerle et al. (2001) and Bregman et al. (2001, 2006) found evidence for O VI emission in the far-UV (FUV), probing gas at $\sim 10^{5.5}$ K, in the cores of several galaxy clusters, inferring cooling rates well below the cooling flow expectation. These observations were nearly always centered on the nucleus of the central cluster galaxy, where AGN feedback could in fact be heating the gas, causing excess O VI emission.

Here we present new FUV spectroscopy (Section 2) of Abell 1795 (A1795), a nearby, strongly-cooling galaxy cluster (see, e.g., Fabian et al. 2001; Ettori et al. 2002; Ehlert et al. 2014). These spectra were obtained along the southwestern filament, which is observed to be cooling rapidly in the X-ray (Crawford et al. 2005; McDonald et al. 2010; Ehlert et al. 2014), contains warm (10^4 K) ionized (Cowie et al. 1983; Crawford et al. 2005; McDonald & Veilleux 2009) and cold molecular gas (Salomé & Combes 2004; McDonald et al. 2012c), and is rapidly forming stars (∼1 $M_{\odot}$ yr^{-1}; McDonald & Veilleux 2009). With deep FUV spectroscopy, we can estimate the age and metallicity of these newly-formed stars (Section 3), allowing us to determine

[6] Hubble Fellow.

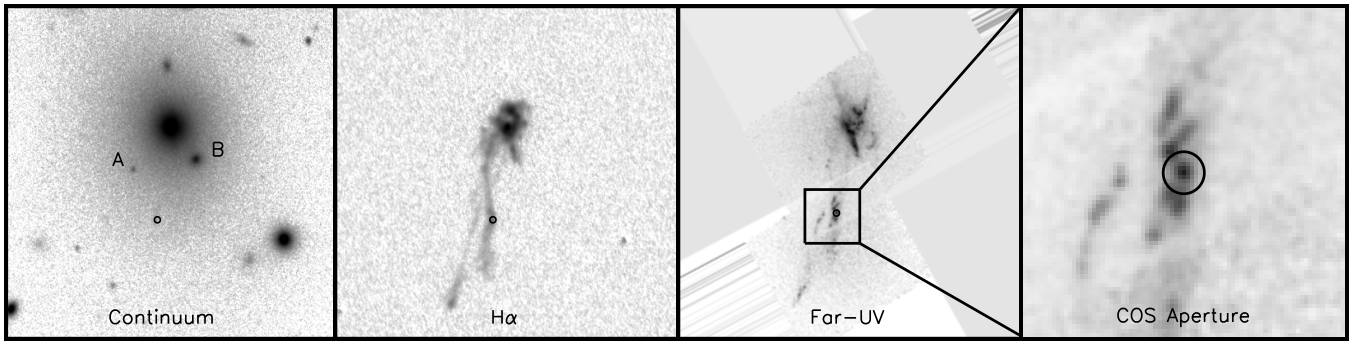

Figure 1. Left: Continuum (∼7000 Å) image of the central galaxy in A1795. Left-center: Hα image showing the twin filaments extending ∼50 kpc to the south of the central galaxy (McDonald & Veilleux 2009). Right-center: Far-UV image from *HST* ACS/SBC (McDonald & Veilleux 2009) showing young stellar populations along the Hα filaments. Right: Zoom-in on the far-UV image, showing the location of the 2.″5 COS aperture. This aperture, which is shown in all four panels, is centered on the brightest UV clump in the western filament. In the leftmost panel, the positions of the two closest galaxies are denoted by A and B. These galaxies are 16 and 21 kpc away in projection from the COS pointing, respectively, implying that any gas/stars in the filaments that originated in the satellite galaxies would have been stripped from these galaxies >26 Myr ago (assuming $v = 800$ km s^{-1}).

if they are forming in situ or have been tidally stripped, while also measuring the O VI emission line flux (Section 4) far from the influence of the central AGN (∼30 kpc). This approach will allow us to link the young stars to the cooling X-ray gas, if that is indeed their origin (Section 5). We will finish, in Section 6, with a discussion of the current state of the cooling flow problem, and how these new data can advance our understanding.

Throughout this Letter, we assume $H_0 = 70$ km s^{-1} Mpc^{-1}, $\Omega_M = 0.27$, and $\Omega_\Lambda = 0.73$.

2. DATA

FUV spectroscopy for this program was acquired using the Cosmic Origins Spectrograph (COS) on the *Hubble Space Telescope* (*HST*) using the G140L grating with $\lambda_{\rm center} = 1280$ Å, which yields a spectral coverage of 1080–1900 Å. The 2.″5 aperture was centered at (α, δ) = 207.°2199, +26°.5873, which corresponds to the peak of both the FUV and Hα emission along the filament (see Figure 1).

COS spectroscopy is simultaneously obtained in "blue" and "red" channels, with respective wavelengths spanning ∼1080–1200 Å and ∼1250–1800 Å for our setup. The gap between 1200 and 1250 Å spans the geocoronal Lyα line (1216 Å). We observe one other strong geocoronal line due to O I at ∼1302.2–1306 Å,[7] which is redward of redshifted Lyβ ($\lambda_{{\rm Ly}\beta} = 1290.8$ Å). We determine the redshift of the spectrum using a joint fit to the Lyβ emission line and two absorption features in the red channel (Si IV λ1394 and C IV λ1548). This fit yields $z = 0.0619 \pm 0.0005$, which is consistent with our optical redshift of $z = 0.0618$ from McDonald et al. (2012b) at the same position along the filament.

3. FUV CONTINUUM: YOUNG STELLAR POPULATIONS

3.1. UV Absorption Indices

To constrain the age and metallicity of the stellar population responsible for the observed FUV continuum in A1795, we use predicted UV absorption line strengths from Maraston et al. (2009, hereafter M09), which are cast in terms of the *International Ultraviolet Explorer* (*IUE*) index system established by Fanelli et al. (1992). The use of an index-based approach helps reduce the uncertainty in our results due to reddening effects, which are most severe at UV wavelengths. Since the M09 models do not consider contributions of other hot stellar phases (e.g., blue horizontal branch), we implicitly assume that the observed FUV emission is entirely due to young (<1 Gyr) stars.

The M09 models come in two flavors: ones based on empirical fitting functions to *IUE* spectra of Milky Way and Magellanic Cloud (MC) stars or others based on theoretical Kurucz spectra. We use the latter here given that they reproduce the ages of MC globular clusters (from color–magnitude diagrams) to within a mean residual of 0.02 ± 0.32 dex (see Appendix C of M09). These models span a semi-regular grid of ages from 1 Myr to 1 Gyr and total metallicities from −1.00 to +0.35 dex with respect to solar.[8] We allow age and metallicity to vary simultaneously in our fits, which follow a maximum likelihood approach. Statistical errors in the best-fit quantities are estimated via Monte Carlo simulations of the measured index errors. Although M09 recommend fitting to all *IUE* indices in the 1000–2000 Å range at once with their theoretical models, we have performed fits to a variety of index combinations, specifically a blue set (BL1302, Si IV, BL1425) and a red set (C IVa, C IV, C IVe, BL1617, BL1664), in order to test the robustness of our results. These results are summarized in Table 1. Overall, we find consistently low ages ($7.5^{+2.5}_{-2.0}$ Myr) and metallicities ($0.4^{+0.2}_{-0.1}$ $Z_\odot$) regardless of which combination of indices we employ.

3.2. Full Spectrum Synthesis

A complementary method of constraining the age and metallicity of the UV-emitting stellar population is to model the full spectrum using synthetic stellar population models. For this, we opt to use the latest version of Starburst99 (v7.0.0; Leitherer et al. 1999),[9] which is, to our knowledge, the only publicly-available stellar population synthesis code with spectral resolution better than 1 Å over 1000 Å < λ < 2000 Å. We restrict this analysis to >1100 Å—at bluer wavelengths, Starburst99 uses empirical stellar spectra which provide a qualitatively-poor fit to the data (see Section 4). We use the latest Geneva tracks, which are only available for solar (Ekström et al. 2012) and 0.14 $Z_\odot$ (Georgy

[7] http://www.stsci.edu/hst/cos/calibration/airglow_table.html

[8] The spacing of the age grid changes from 0.5 Myr, to 5 Myr, to 50 Myr in the intervals 1 Myr-10 Myr, 10 Myr-0.1 Gyr, and 0.1–1.0 Gyr, respectively. On the other hand, the models are spaced at 0.1 dex intervals in terms of metallicity, except the +0.35 dex models, which are offset by 0.15 dex from the +0.20 dex models.

[9] http://www.stsci.edu/science/starburst99/docs/default.htm

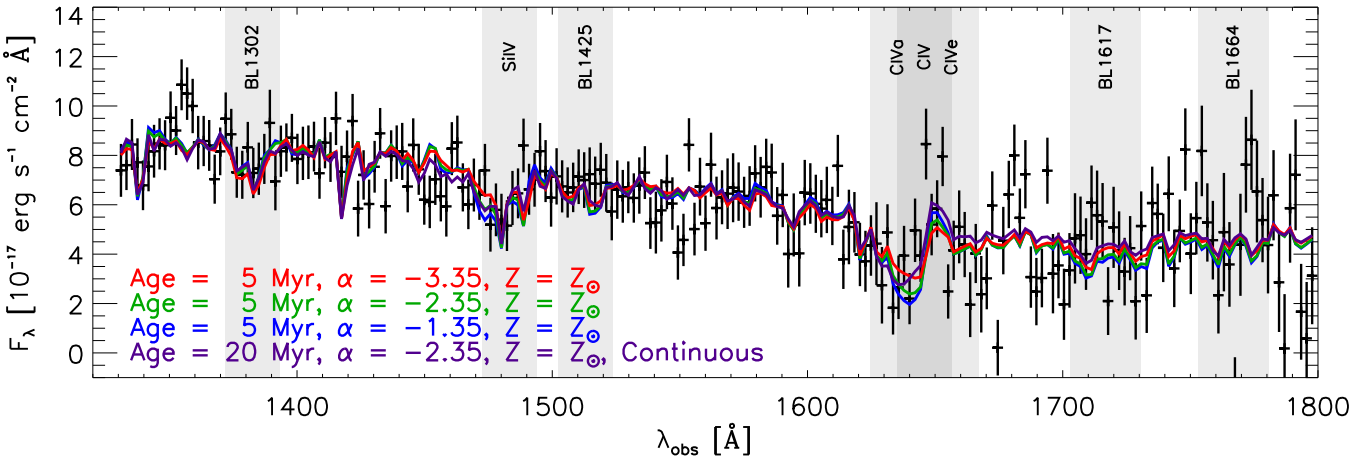

Figure 2. Far-UV spectrum from the red channel of our *HST*-COS observation. This spectrum has been binned in wavelength by a factor of 27 (2.2 Å) in order to improve signal-to-noise. Vertical gray bands correspond to spectral indices as defined by Fanelli et al. (1992). Overplotted are various models generated with Starburst99 (Leitherer et al. 1999) using the latest stellar tracks from Ekström et al. (2012) and Georgy et al. (2013), demonstrating the overall quality of these fits to the data.

(A color version of this figure is available in the online journal.)

Table 1
Stellar Age and Metallicity from UV Absorption Line Indices

Indices	Age [Myr]	$\log_{10}(Z)$ [$Z_\odot$]
BL1302, Si IV, BL1425, C IVa, C IV, C IVe, BL1617, BL1664	$7.5^{+2.5}_{-2.0}$	$-0.4^{+0.2}_{-0.1}$
Si IV, BL1425, C IVa, C IV, C IVe, BL1617, BL1664	$10.0^{+10.0}_{-4.5}$	$-0.2^{+0.2}_{-0.2}$
BL1302, BL1425, C IVa, C IV, C IVe, BL1617, BL1664	$7.5^{+2.5}_{-2.0}$	$-0.4^{+0.2}_{-0.3}$
BL1302, Si IV, C IVa, C IV, C IVe, BL1617, BL1664	$7.5^{+2.0}_{-4.0}$	$-0.4^{+0.2}_{-0.1}$
BL1302, Si IV, BL1425, C IV, C IVe, BL1617, BL1664	$9.5^{+0.5}_{-2.0}$	$-0.5^{+0.1}_{-0.1}$
BL1302, Si IV, BL1425, C IVa, C IVe, BL1617, BL1664	$3.0^{+4.0}_{-1.0}$	$-0.1^{+0.5}_{-0.3}$
BL1302, Si IV, BL1425, C IVa, C IV, BL1617, BL1664	$6.5^{+3.5}_{-3.0}$	$-0.4^{+0.2}_{-0.1}$
BL1302, Si IV, BL1425, C IVa, C IV, C IVe, BL1664	$7.5^{+2.5}_{-2.0}$	$-0.4^{+0.1}_{-0.1}$
BL1302, Si IV, BL1425, C IVa, C IV, C IVe, BL1617	$7.5^{+2.5}_{-2.0}$	$-0.4^{+0.2}_{-0.1}$

Notes. All uncertainties are 1σ. See Maraston et al. (2009) for a discussion of far-UV absorption indices.

et al. 2013) metallicities. We explore three different initial mass functions (IMFs): Salpeter (Salpeter 1955, $\alpha = -2.35$), with top-heavy ($\alpha = -1.35$) and top-light ($\alpha = -3.35$) variants. For each choice of metallicity and IMF, we generate synthetic spectra assuming either a burst or continuous star formation, over timescales of 50 Myr. These model spectra are fit to the data, allowing the normalization, redshift, and reddening to vary, with a lower limit of the Galactic value imposed on the reddening (Schlegel et al. 1998).

Figures 2 and 3 show the results of this exercise. In Figure 2 we compare several best-fitting models to the data, demonstrating the overall quality of these fits. These synthetic spectra are able to adequately fit the various absorption features discussed in Section 3.1. The goodness-of-fit ($\chi^2_{\rm dof}$) is shown in Figure 3 as a function of age, metallicity, and IMF, for both instantaneous and continuous star formation. All starburst models favor a relatively young population, with the majority showing minima at ages of 5 Myr. The continuous star formation models prefer either a Salpeter IMF, with ages >10 Myr or a younger top-light stellar population. As is also the case for the burst-like models, the distinguishing power between IMFs comes from the C IV feature (see Figure 2), which is likely contaminated by emission. Qualitatively, all three choices of IMF perform equally well in fitting the spectrum over the range 1220 Å $< \lambda_{\rm rest} <$ 1700 Å.

This analysis corroborates the results from FUV line indices (Section 3.1), demonstrating that the best-fitting stellar population is one that is either currently forming stars, or ceased very recently ($\lesssim$10 Myr ago).

4. FUV EMISSION LINES: PROBING $10^{5.5}$ K GAS WITH O VI

In Figure 4 we show the blue side (<1200 Å) of the spectrum. These data are significantly noisier than the red channels, and suffer from airglow emission and Galactic H_2 absorption to a higher degree. Despite this, there is evidence for emission at redshifted O VI λ1038 in the binned spectrum (upper panel of Figure 4). The spectrum of Galactic H_2 absorption from McCandliss (2003) shows strong absorption at the same wavelength as redshifted O VI λ1032, which likely explains the lack of emission from the bluer line in this doublet, which should have a factor of 2 higher flux. At these wavelengths, Starburst99 relies on empirical stellar spectra (see Section 3) which provide a relatively poor fit to the data, so we opt to model the continuum spectrum by performing a median smoothing over a 2.4 Å ($\sim$650 km s^{-1}) window, which should be significantly wider than any emission lines. The residual spectrum with this model subtracted is shown in the lower panel of Figure 4.

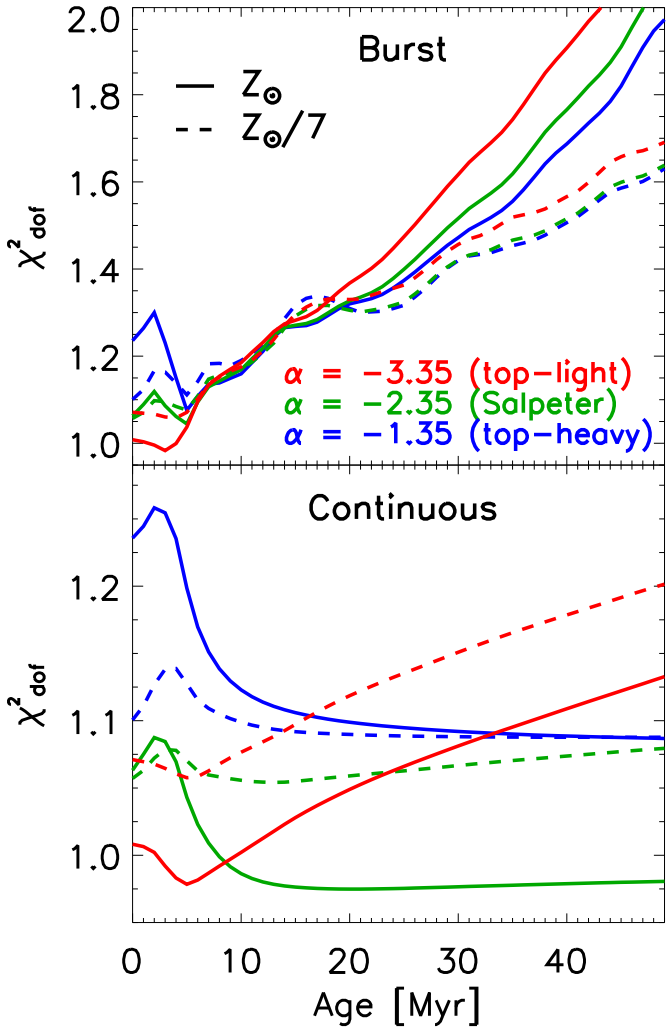

Figure 3. Goodness-of-fit (χ^2_{dof}) as a function of age for instantaneous (upper panel) and continuous (lower panel) star formation. For all choices of IMF and metallicity, the data are well-represented by either a young ($\lesssim$10 Myr) stellar population or ongoing star formation.

(A color version of this figure is available in the online journal.)

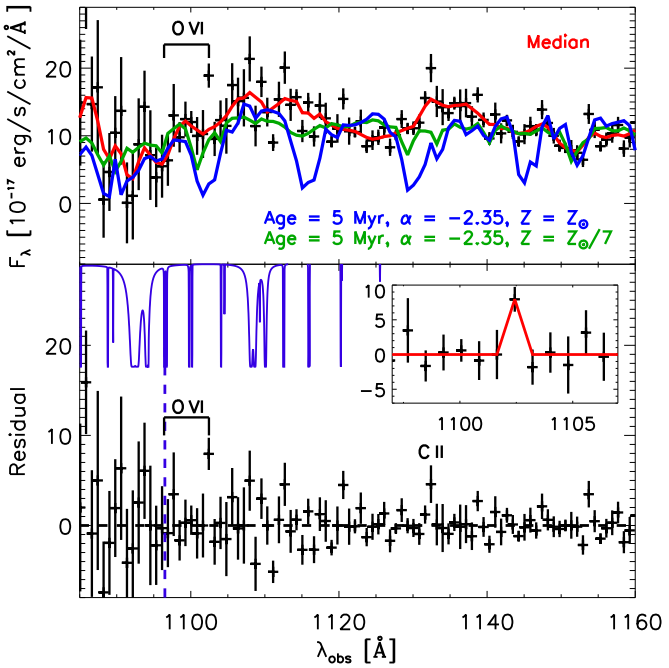

Figure 4. Upper panel: Far-UV spectrum from the blue channel of our *HST*-COS observation. Here, we show the binned (0.8 Å) data along with stellar population synthesis models from Starburst99 (Leitherer et al. 1999) and a median continuum spectrum computed with a 2.4 Å smoothing window. At these wavelengths Starburst99 only provides empirical models, which yield poor fits to the data (note that the red channels are well-fit by a solar-metallicity model; Figure 2). Lower panel: Residual spectrum, with the median continuum level subtracted. The expected location of the O VI λλ1032,1038 doublet is highlighted. In purple, we plot the spectrum of Galactic H_2 absorption from McCandliss (2003), which shows that the bluer O VI λ1032 line is most likely being absorbed by molecular gas in our galaxy. The correspondence between a saturated absorption line and the O VI λ1032 line is highlighted by a vertical dashed line. We detect the redder, unabsorbed line at >4σ significance, as shown in the inset, with a velocity width of $\lesssim$0.7 Å ($\lesssim$90 km s^{-1}).

(A color version of this figure is available in the online journal.)

Assuming a linewidth of 0.43 Å (σ = 50 km s^{-1}), based on the Hα velocity dispersion (McDonald et al. 2012b), we measure a flux of $f_{O\,VI} = 4.0 \pm 0.9 \times 10^{-17}$ erg s^{-1} cm^{-2} in the redder line of the O VI doublet (>4σ detection). While the statistical significance of this line is low, we note that it is the most statistically significant deviation over the entire blue spectrum. The fact that this deviation is at the wavelength that we expect to find redshifted O VI further strengthens the significance of the detection. The width of this line is $\lesssim$0.7 Å or $\lesssim$90 km s^{-1}.

5. INTERPRETATION: ONGOING STAR FORMATION IN CONDENSING FILAMENTS OF INTRACLUSTER GAS

Given the high-ionization energy of the O VI transition (138.1 eV), it not likely to be due to the same process(es) responsible for the low-ionization Hα emission (Figure 1). The original detection of O VI in the center of A1795 by Bregman et al. (2006) was taken as evidence for cooling of the ICM. Alternatively, Sparks et al. (2012) recently invoked an evaporation scenario to explain the filamentary coronal emission in the core of the Virgo cluster. In the latter scenario, the hypothesis is that cool gas has been stripped from nearby gas-rich galaxies and is being heated via conduction by the hot ICM. The lack of stars in the filaments surrounding M87 was offered as further evidence of this scenario.

The detection of young ($\lesssim$10 Myr) stars and cold molecular gas (McDonald et al. 2012c) in the filaments of A1795 favors the scenario in which gas is condensing and stars are forming in situ. If, instead, the cool gas originated in a nearby galaxy, it would have been stripped *at least* 26 Myr ago, given the distance to the nearest satellite galaxy (21 kpc; Figure 1) and the typical galaxy velocities in the core of A1795 (~800 km s^{-1}). Assuming the stars are forming in situ, it seems unlikely that the filamentary gas is simultaneously condensing (into stars) and evaporating (causing coronal emission)—the simplest explanation is that the hot intracluster gas is cooling through the O VI transition and into molecular gas, before ultimately forming stars. The agreement between the measured metallicity of the stars ($0.4^{+0.2}_{-0.1}$ $Z_\odot$; Table 1) and the cooling ICM at the same position ($0.5^{+0.3}_{-0.2}$ $Z_\odot$; Ehlert et al. 2014) further supports this scenario.

If we assume that the O VI λ1038 emission is due to cooling intracluster gas, we can estimate the cooling rate following Edgar & Chevalier (1986) and Voit et al. (1994). The inferred cooling rate can vary by a factor of ~1.6 depending on if the cooling proceeds isobarically or isochorically. Based on very deep X-ray data of the cooling filament (Ehlert et al. 2014), we estimate the sound-crossing time at the location of the COS

aperture to be ∼2–5 Myr and the cooling time to be ∼2 Myr (assuming $n_e \sim 1$ cm^{-3}). Thus, it is unclear exactly how the cooling will proceed. Based on the measured O VI λ1038 flux, and following Edgar & Chevalier (1986), we estimate a cooling rate of 0.85 ± 0.15 (stat) $\pm$ 0.20 (sys) $M_\odot$ yr^{-1}, where the systematic uncertainty includes expectation for isobaric ($1.0 \pm 0.2\ M_\odot$ yr^{-1}) and isochoric ($0.7 \pm 0.2\ M_\odot$ yr^{-1}) cooling.

This cooling rate, which probes $\sim 10^{5.5}$ K gas, can be compared to both the X-ray cooling rate and the star formation rate, which probe the hot ($\sim 10^7$ K) and cold (∼10 K) extremes, respectively. We estimate the classical cooling rate ($\dot{M}_X = 2L_X \mu m_p / 5kT$) within the COS aperture to be $\sim 1\ M_\odot$ yr^{-1}, assuming that, on small (<kiloparsec) scales, the cooling ICM is similar in morphology (clumpiness) to the UV continuum. Based on our stellar population modeling (Section 3.2), we estimate an extinction-corrected star formation rate (assuming continuous star formation) within the COS aperture of $0.11 \pm 0.02\ M_\odot$ yr^{-1}. This suggests that 13^{+3}_{-2}% of the gas cooling through $10^{5.5}$ K is converted to stars.

Alternatively, some fraction of the O VI emission could come from a mixing layer, where hot electrons from the ICM penetrate the cold filaments, following Fabian et al. (2011)—correcting for this would raise the inferred star formation efficiency. However, we do not find an excess of optical line emission above the expectation given the UV continuum level, as is observed in NGC 1275, suggesting that these effects are small in the filaments of A1795.

For comparison, Bregman et al. (2006) find a total O VI-derived cooling rate of $42 \pm 9\ M_\odot$ yr^{-1} over the full core of A1795, while the extinction-corrected star formation rate (assuming $\langle E(B-V) \rangle = 0.1$; McDonald et al. 2012b) over the same area is only $5.2\ M_\odot$ yr^{-1} (McDonald & Veilleux 2009). This corresponds to an efficiency of forming stars out of the $10^{5.5}$ K gas of 12^{+4}_{-2}%. This is also comparable to the star formation efficiency found by McDonald et al. (2011) of 14^{+18}_{-8}% based on X-ray spectroscopy and UV photometry.

6. IMPLICATIONS FOR THE COOLING FLOW PROBLEM

Given that cooling flows are found to be ∼1% efficient at converting the cooling ICM into stars (e.g., O'Dea et al. 2008), it is important to understand at what temperatures the bulk of the gas is held up. Assuming that the IMF does indeed follow Salpeter (1955), we find, for the filaments in A1795 (where the effects of AGN feedback should be minimized), that the cooling efficiency at high temperatures is of order 100% ($\epsilon_{\rm hot} \equiv \dot{M}_{\rm O\,VI}/\dot{M}_X \sim 0.7$–1.0), while the star formation efficiency is low ($\epsilon_{\rm cold} \equiv {\rm SFR}/\dot{M}_{\rm O\,VI} \sim 0.11$–0.16). In contrast, Bregman et al. (2001) found, using O VI observations from *FUSE*, that $\epsilon_{\rm hot}$ was of order 10% *over the full cluster core* for A1795, A2597, and Perseus. This suggests that the cooling flow problem may be divided into two separate inefficiencies.

1. $\epsilon_{\rm hot} \sim 0.1$: globally inefficient cooling at high temperatures (10^7 K → 10^5 K), due to some large-scale feedback source (e.g., AGN);
2. $\epsilon_{\rm cold} \sim 0.1$: locally inefficient cooling at low temperatures (10^5 K → stars), manifesting as inefficient star formation.

The latter, which we quantify here and in McDonald et al. (2011), may be low due to conduction suppressing cooling at low temperatures. For comparison, star clusters in our Galaxy have typical star formation efficiencies of ∼8%–30% (Lada & Lada 2003)—in principle, star formation embedded in a hot plasma should proceed less efficiently.

SUMMARY

We present deep FUV spectroscopy of a cooling filament in A1795, obtained using the COS on *HST*. These data allow us to simultaneously probe the young stellar populations and the intermediate temperature ($10^{5.5}$ K) gas. We find evidence for ongoing, in situ star formation, which suggests that the cool gas in these filaments was *not* stripped from an infalling galaxy. The detection of O VI emission suggests that this star formation is being fueled by condensing intracluster gas, and that the cooling is proceeding efficiently at high temperatures, contrary to what is observed on large scales in cluster cores. We propose a scenario where the two orders of magnitude disagreement between luminosity-based X-ray cooling rates and star formation in cluster cores is due to a combination of globally-inefficient cooling at high temperatures ($\epsilon_{\rm hot} \sim 0.1$; e.g., AGN feedback) and locally-inefficient star formation at low temperatures ($\epsilon_{\rm cold} \sim 0.1$).

M.M. acknowledges support provided by NASA through a Hubble Fellowship grant from STScI and through *HST* GO-12992 contract NAS5-26555. S.V. acknowledges support from a Senior NPP Award held at NASA-GSFC. S.E. acknowledges support from SAO subcontract SV2-82023 under NASA contract NAS8-03060.

REFERENCES

Allen, S. W. 1995, MNRAS, 276, 947
Bregman, J. N., Fabian, A. C., Miller, E. D., & Irwin, J. A. 2006, ApJ, 642, 746
Bregman, J. N., Miller, E. D., & Irwin, J. A. 2001, ApJL, 553, L125
Churazov, E., Brüggen, M., Kaiser, C. R., Böhringer, H., & Forman, W. 2001, ApJ, 554, 261
Cowie, L. L., Hu, E. M., Jenkins, E. B., & York, D. G. 1983, ApJ, 272, 29
Crawford, C. S., Sanders, J. S., & Fabian, A. C. 2005, MNRAS, 361, 17
Edgar, R. J., & Chevalier, R. A. 1986, ApJL, 310, L27
Edge, A. C. 2001, MNRAS, 328, 762
Edge, A. C., Wilman, R. J., Johnstone, R. M., et al. 2002, MNRAS, 337, 49
Ehlert, S., McDonald, M., Miller, E. D., David, L. P., & Bautz, M. W. 2014, arXiv:1406.4352
Ekström, S., Georgy, C., Eggenberger, P., et al. 2012, A&A, 537, A146
Ettori, S., Fabian, A. C., Allen, S. W., & Johnstone, R. M. 2002, MNRAS, 331, 635
Fabian, A. C. 1994, ARA&A, 32, 277
Fabian, A. C. 2012, ARA&A, 50, 455
Fabian, A. C., Sanders, J. S., Ettori, S., et al. 2001, MNRAS, 321, L33
Fabian, A. C., Sanders, J. S., Williams, R. J. R., et al. 2011, MNRAS, 417, 172
Fanelli, M. N., O'Connell, R. W., Burstein, D., & Wu, C.-C. 1992, ApJS, 82, 197
Georgy, C., Ekström, S., Eggenberger, P., et al. 2013, A&A, 558, A103
Hatch, N. A., Crawford, C. S., Fabian, A. C., & Johnstone, R. M. 2005, MNRAS, 358, 765
Hicks, A. K., & Mushotzky, R. 2005, ApJL, 635, L9
Hicks, A. K., Mushotzky, R., & Donahue, M. 2010, ApJ, 719, 1844
Johnstone, R. M., Fabian, A. C., & Nulsen, P. E. J. 1987, MNRAS, 224, 75
Lada, C. J., & Lada, E. A. 2003, ARA&A, 41, 57
Leitherer, C., Schaerer, D., Goldader, J. D., et al. 1999, ApJS, 123, 3
Maraston, C., Nieves Colmenárez, L., Bender, R., & Thomas, D. 2009, A&A, 493, 425
McCandliss, S. R. 2003, PASP, 115, 651
McCourt, M., Sharma, P., Quataert, E., & Parrish, I. J. 2012, MNRAS, 419, 3319
McDonald, M., Bayliss, M., Benson, B. A., et al. 2012a, Natur, 488, 349
McDonald, M., & Veilleux, S. 2009, ApJL, 703, L172
McDonald, M., Veilleux, S., & Rupke, D. S. N. 2012b, ApJ, 746, 153
McDonald, M., Veilleux, S., Rupke, D. S. N., & Mushotzky, R. 2010, ApJ, 721, 1262
McDonald, M., Veilleux, S., Rupke, D. S. N., Mushotzky, R., & Reynolds, C. 2011, ApJ, 734, 95
McDonald, M., Wei, L. H., & Veilleux, S. 2012c, ApJL, 755, L24
McNamara, B. R., & Nulsen, P. E. J. 2012, NJPh, 14, 055023

McNamara, B. R., & O'Connell, R. W. 1989, AJ, 98, 2018
McNamara, B. R., Rafferty, D. A., Bîrzan, L., et al. 2006, ApJ, 648, 164
O'Dea, C. P., Baum, S. A., Privon, G., et al. 2008, ApJ, 681, 1035
Oegerle, W. R., Cowie, L., Davidsen, A., et al. 2001, ApJ, 560, 187
Peterson, J. R., & Fabian, A. C. 2006, PhR, 427, 1
Peterson, J. R., Kahn, S. M., Paerels, F. B. S., et al. 2003, ApJ, 590, 207
Rafferty, D. A., McNamara, B. R., & Nulsen, P. E. J. 2008, ApJ, 687, 899
Rafferty, D. A., McNamara, B. R., Nulsen, P. E. J., & Wise, M. W. 2006, ApJ, 652, 216
Salomé, P., & Combes, F. 2003, A&A, 412, 657
Salomé, P., & Combes, F. 2004, A&A, 415, L1
Salomé, P., Combes, F., Revaz, Y., et al. 2011, A&A, 531, A85
Salpeter, E. E. 1955, ApJ, 121, 161
Sanders, J. S., & Fabian, A. C. 2011, MNRAS, 412, L35
Sanders, J. S., Fabian, A. C., Smith, R. K., & Peterson, J. R. 2010, MNRAS, 402, L11
Schlegel, D. J., Finkbeiner, D. P., & Davis, M. 1998, ApJ, 500, 525
Sparks, W. B., Pringle, J. E., Carswell, R. F., et al. 2012, ApJL, 750, L5
Voit, G. M., Donahue, M., & Slavin, J. D. 1994, ApJS, 95, 87